Available online at www.sciencedirect.com

ScienceDirect

IFAC Papers Online CONFERENCE PAPER ARCHIVE

IFAC PapersOnLine 50-1 (2017) 2131–2136

A Third Harmonic Injected PWM Scheme with Partial Feedback Linearizing Controller for Grid-Connected Ultracapacitor System

S.M. Mohiuddin * **M.A. Mahmud** ** **H.R. Pota** *

* *School of Engineering and Information Technology, The University of New South Wales, Canberra, ACT 2610, Australia (e-mail: Sheik.Mohiuddin@student.adfa.edu.au, h.pota@adfa.edu.au, a.haruni@adfa.edu.au).*

** *School of Engineering, Deakin University, Geelong Waurn Ponds Campus, Australia (e-mail: apel.mahmud@deakin.edu.au)*

Abstract: In this paper, a high-efficiency third harmonic injected pulse width modulation (PWM) scheme is presented for an ultracapacitor-based energy storage system (UCESS). Also, a nonlinear partial feedback linearizing controller is used with the proposed third harmonic injected PWM scheme where the main control objectives are to regulate the active and reactive power injection into the grid from the UCESS. The dynamical model of the grid-connected UCESS is developed from the electrical equivalent circuit, where the grid connection is accomplished through a three-phase voltage source converter (VSC). The grid current components corresponding to both active and reactive power are regulated through the proposed control action. Since the proposed control scheme reduces the order of the original UCESS, the stability of remaining dynamics (i.e., internal dynamics) is investigated before implementing the proposed controller. The implementation of the proposed control scheme also requires the injection of the third harmonic externally as the incorporation of this harmonic during the modeling does not affect the transient and steady-state characteristics of the system. A test distribution system is considered to justify the performance of the proposed scheme through the simulation results. The simulation results show the superiority of the proposed controller as compared to a finely-tuned proportion integral (PI) controller.

Keywords: Ultracapacitor, energy storage, partial feedback linearizing controller, third harmonic injected PWM.

1. INTRODUCTION

The integration of renewable energy sources (RESs) has significantly increased in recent years for a number of technical, environmental and economical benefits they offer to the utilities as well as the consumers (Mahmud et al., 2013). Since RESs depend on the environmental conditions which are intermittent in nature, energy storage systems (ESSs) are required to supply power in the case of emergency as well as to mitigate the power fluctuations (Mahmud et al., 2014a). An ultracapcitor (UC) based ESS is considered in this paper for providing both active and reactive power support to the grid.

The ultracapacitor-based energy storage systems (UCESSs) are now being used as a powerful energy storage solutions in power system applications (Schneuwly, 2006). Compared to other energy storage devices the UC has some distinct advantages such as it has no moving parts, no chemical reaction is required for its functions, can efficiently operate throughout the life with little or even no maintenance (Molina and Mercado, 2008). The UC has high power density, fast access to the stored energy, rapid charging and discharging capability, 10^6 times higher charge/discharge cycle compared to a battery, very low leakage currents, and can operate over a wide range of temperature -40^oC to 85^oC (Sahay and Dwivedi, 2009). Thus, the UC can play a vital role for network support (active and reactive power support) in power systems.

A cluster of distributed generators (DGs), energy storage devices and the associated loads interconnected as a single entity form a microgrid. Microgrids can operate autonomously or in conjunction with the grid with the implementation of suitable control methods. The DGs and ESSs, in most of the cases generate or store DC power and therefore some interfacing units are required to integrate these devices into the grid. These interfacing units are based on power electronics which have nonlinear characteristics and make the microgrid as an inertialess and/or a low-inertia grid (Mahmud et al., 2014a). Due to the lack of inertia the frequency and voltage stability become critical with the variation of intermittent RESs which will further lead to the active and reactive power mismatches within the system. The nonlinearity of switching devices increases when power from the RESs fluctuates along with the variations in load demand. Under these varying circumstances, linear controllers are unable to provide appropriate active and reactive power support (Mahmud et al., 2014a). Thus, the controllers need to be designed based on a model which can capture the aforementioned nonlinearities while ensuring appropriate active and reactive power support.

In a pulse width modulation (PWM) scheme, the switch cell has to withstand the whole DC-side voltage during off state and therefore, the design of the switches is a critical issue. Furthermore, the cost of the switches increases with the increase in voltage requirements and the switches may fail to fulfill all requirements when the voltage levels are higher. This issue can be resolved utilizing a high-efficiency third harmonic injected PWM technique. Employing third harmonic injected PWM scheme, for a given AC-side voltage level the DC-bus voltage can be reduced by around 13 percent or for the same DC-bus voltage level the AC-side

10.1016/j.ifacol.2017.08.586

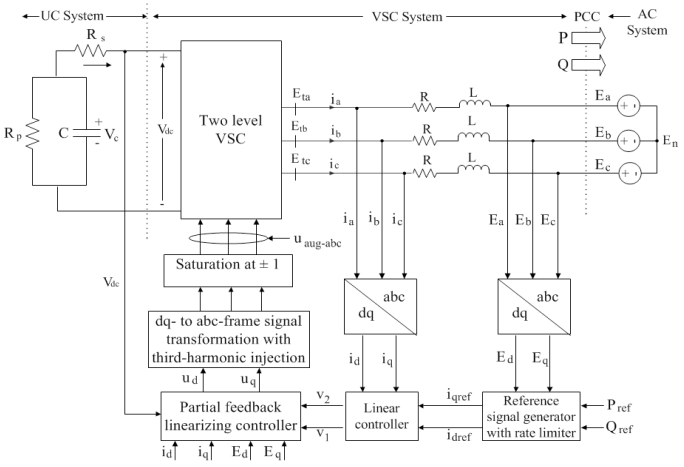

Fig. 1. Schematic diagram of grid-connected ultracapacitor-based energy storage systems utilizing third-harmonic injected PWM.

voltage can be increased by about 15 percent (Yazdani and Iravani, 2010).

The UC with a bidirectional DC-DC converter is used as a backup storage element to smooth the power fluctuations in a hybrid energy conversion system (Abdullah et al., 2014). A two-level control (supervisory and sliding mode control) strategy is implemented in (Mor et al., 2015), where the DC-DC converter is only capable of sharing active power from the sources. The UC-based energy storage system is considered in (Khosravi et al., 2015; Singo et al., 2008) for a standalone PV system. The UC with a flyback converter is used to reduce the transients in a hybrid fuel cell (FC)-UC system (Sami et al., 2013). However, the reactive power supply capability from the UCESS remained unexplored in (Abdullah et al., 2014; Mor et al., 2015; Singo et al., 2008; Khosravi et al., 2015; Sami et al., 2013). UC can be also coupled with distribution static synchronous compensator (DSTATCOM) to improve power quality in distribution networks (Molina and Mercado, 2008). A model predictive approach is proposed in (Bambang et al., 2014) for energy management in a hybrid fuel cell/battery/supercapacitor based power system. The model predictive controller has several drawbacks such as difficulties with the operation, high maintenance cost, and lack of flexibility. The UC with an active power filter (APF) is integrated in (Somayajula and Crow, 2015) to reduce the fluctuations in active and reactive power supply. In (Somayajula and Crow, 2015), PI controllers are used to control the current components which suffers from several limitations such as slow convergence, poor disturbance rejection capability, steady-state error for tracking sinusoidal reference, and adjustment of gains with the changes in atmospheric conditions (Mahmud et al., 2014c; Jang et al., 2013).

The effect of injecting third harmonic on the dynamics and steady-state characteristics of a grid-connected UCESS is investigated in this paper. The partial feedback linearization technique is applied to generate control signals for the pupose of the third harmonic injection. The active and reactive power injected into the grid are controlled through the regulation of dq-axes components of the grid current. The stability of internal dynamics of UCESSs is also ensured. Finally, the third harmonic injected PWM scheme is implemented along with the control signals obtained through the partial feedback linearization technique. Since the proposed linearization scheme is independent of the operating points, the stability of the grid-connected UCESS is maintained over a wide operating region.

2. DYNAMIC MODELING OF THIRD-HARMONIC INJECTED UCESSS

The UC has the capability of storing and releasing energy through charging and discharging, respectively. The dynamical model of UCESS can be developed based on the classical electrical equivalent circuit of UC (Uzunoglu and Alam, 2006). Fig. 1 shows, the classical equivalent circuit of UC is interfaced to the three-phase grid through a VSC; where C represents the capacitance, the series resistance R_s represents the charging and discharging resistances, and the resistance R_p represents the self-discharging losses of the UC. The switching losses of the VSC are neglected. Each phase of the VSC is interfaced to the corresponding phase of the grid through a series RL branch. Initially, it has been assumed that the grid is infinitely stiff, balanced, and sinusoidal with constant frequency (Yazdani and Iravani, 2010).

2.1 Space-phasor representation of the UCESS system

In this subsection, the UCESS system shown in Fig. 1 is represented in the space-phasor form. To do this, the following equation can be written for the DC-side of this circuit:

$$\frac{dV_{\rm c}}{dt} = -\frac{V_{\rm c}}{R_{\rm p}C} - \frac{i_{\rm dc}}{C} \tag{1}$$

Similarly, the following equations can be obtained from the AC-side:

$$L\frac{di_{\rm a}}{dt} = -Ri_{\rm a} + E_{\rm ta} - E_{\rm a} - E_{\rm n} \tag{2a}$$

$$L\frac{di_{\rm b}}{dt} = -Ri_{\rm b} + E_{\rm tb} - E_{\rm b} - E_{\rm n} \tag{2b}$$

$$L\frac{di_{\rm c}}{dt} = -Ri_{\rm c} + E_{\rm tc} - E_{\rm c} - E_{\rm n} \tag{2c}$$

For the two-level VSC the AC-side terminal voltages can be represented as:

$$E_{\rm ta}(t) = \frac{V_{\rm dc}}{2}u_{\rm a}(t), \quad E_{\rm tb}(t) = \frac{V_{\rm dc}}{2}u_{\rm b}(t) \quad \text{and} \quad E_{\rm tc}(t) = \frac{V_{\rm dc}}{2}u_{\rm c}(t) \tag{3}$$

where the modulating signals $u_{\rm abc}(t)$ are a balanced three-phase signal which can be expressed as follows:

$$u_{\rm a}(t) = \hat{u}\cos[\epsilon(t)], \quad u_{\rm b}(t) = \hat{u}\cos[\epsilon(t) - \frac{2\pi}{3}] \quad \text{and} \quad u_{\rm c}(t) = \hat{u}\cos[\epsilon(t) - \frac{4\pi}{3}] \tag{4}$$

where $\hat{u}$ represents the amplitude of the modulating signals $u_{\rm abc}(t)$ and the frequency and phase angle information of the modulating signals are expressed by $\epsilon(t)$. When the third-harmonic injected PWM is implemented the modulating signals are modified as follows:

$$u_{\text{aug-a}} = \hat{u}\cos\epsilon - \frac{1}{6}\hat{u}\cos 3\epsilon \tag{5a}$$

$$u_{\text{aug-b}} = \hat{u}\cos\left(\epsilon - \frac{2\pi}{3}\right) - \frac{1}{6}\hat{u}\cos\left(3\epsilon - \frac{2\pi}{3}\right) \tag{5b}$$

$$u_{\text{aug-c}} = \hat{u}\cos\left(\epsilon - \frac{4\pi}{3}\right) - \frac{1}{6}\hat{u}\cos\left(3\epsilon - \frac{4\pi}{3}\right) \tag{5c}$$

Thus $u_{\text{aug-abc}}$ as the modulating signals and using equation (3), the AC-side terminal voltages of the VSC can be expressed as:

$$E_{\text{taug-a}} = \hat{u}\frac{V_{\text{dc}}}{2}\cos\epsilon - \hat{u}\frac{V_{\text{dc}}}{12}\cos 3\epsilon \quad (6a)$$

$$E_{\text{taug-b}} = \hat{u}\frac{V_{\text{dc}}}{2}\cos\left(\epsilon - \frac{2\pi}{3}\right) - \hat{u}\frac{V_{\text{dc}}}{12}\cos\left(3\epsilon - \frac{2\pi}{3}\right) \quad (6b)$$

$$E_{\text{taug-c}} = \hat{u}\frac{V_{\text{dc}}}{2}\cos\left(\epsilon - \frac{4\pi}{3}\right) - \hat{u}\frac{V_{\text{dc}}}{12}\cos\left(3\epsilon - \frac{4\pi}{3}\right) \quad (6c)$$

Summation of equation (6) yields:

$$E_{\text{taug-a}} + E_{\text{taug-b}} + E_{\text{taug-c}} = -\hat{u}\frac{V_{\text{dc}}}{12}\Big[\cos 3\epsilon - \cos\left(3\epsilon - \frac{2\pi}{3}\right) - \cos\left(3\epsilon - \frac{4\pi}{3}\right)\Big] \quad (7)$$

Similarly, adding both sides of equation (2) one can write:

$$L\frac{d}{dt}(\imath_a + \imath_b + \imath_c) = -R(\imath_a + \imath_b + \imath_c) + (E_{\text{taug-a}} + E_{\text{taug-b}} + E_{\text{taug-c}}) - (E_{\text{a}} + E_{\text{b}} + E_{\text{c}}) - 3E_{\text{n}} \quad (8)$$

Since the AC-side of the VSC interface is a three-wire connection, $(\imath_a + \imath_b + \imath_c) \equiv 0$. Thus, substitution of $(E_{\text{taug-a}}+E_{\text{taug-b}}+E_{\text{taug-c}})$ from equation (7) into equation (8) will yield

$$E_{\text{n}} = -\hat{u}\frac{V_{\text{dc}}}{36}\Big[\cos 3\epsilon - \cos\left(3\epsilon - \frac{2\pi}{3}\right) - \cos\left(3\epsilon - \frac{4\pi}{3}\right)\Big] \quad (9)$$

Equation (9) indicates that the third harmonic component of the PWM modulating signal appears at the AC-side neutral point. The same would be true if the modulating signal included any other triple-n harmonic component. Inserting the values of $E_{\text{taug-abc}}$ from equation (6) and E_n from equation (9) into equation (2), one can derive:

$$L\frac{d\imath_{\text{a}}}{dt} = -R\imath_{\text{a}} + \hat{u}\frac{V_{\text{dc}}}{2}\cos\epsilon - E_{\text{a}} \quad (10a)$$

$$L\frac{d\imath_{\text{b}}}{dt} = -R\imath_{\text{b}} + \hat{u}\frac{V_{\text{dc}}}{2}\cos\left(\epsilon - \frac{2\pi}{3}\right) - E_{\text{b}} \quad (10b)$$

$$L\frac{d\imath_{\text{c}}}{dt} = -R\imath_{\text{c}} + \hat{u}\frac{V_{\text{dc}}}{2}\cos\left(\epsilon - \frac{4\pi}{3}\right) - E_{\text{c}} \quad (10c)$$

Thus from equations (4) and (10), it can be written that

$$L\frac{d\imath_{\text{a}}}{dt} = -R\imath_{\text{a}} + \frac{V_{\text{dc}}}{2}u_{\text{a}} - E_{\text{a}}, \quad L\frac{d\imath_{\text{b}}}{dt} = -R\imath_{\text{b}} + \frac{V_{\text{dc}}}{2}u_{\text{b}} - E_{\text{b}} \quad \text{and} \quad L\frac{d\imath_{\text{c}}}{dt} = -R\imath_{\text{c}} + \frac{V_{\text{dc}}}{2}u_{\text{c}} - E_{\text{c}} \quad (11)$$

From equation (11), it is clear that the third harmonic injected PWM approach has no impact on the transients and steady-state characteristics of the system. Thus the space-phasor form of the UCESS represented by equations (1) and (11) can be written as follows (Yazdani and Iravani, 2010):

$$\frac{dV_{\text{c}}}{dt} = -\frac{V_{\text{c}}}{R_{\text{p}}C} - \frac{3}{4C}\boldsymbol{u\imath} \quad (12)$$

$$L\frac{d\boldsymbol{\imath}}{dt} = -R\boldsymbol{\imath} + \frac{V_{\text{dc}}}{2}\boldsymbol{u} - \boldsymbol{E} \quad (13)$$

2.2 dq-frame representation of the UCESS model

To simplify the analysis and the controller design tasks, the variables in space-phasor are projected on a synchronously rotating dq-frame. Utilizing the relation $\bar{f} = (f_d + jf_q)e^{j\rho}$ where $\bar{f}$ represents the space-phasor and f_d and f_q represents the space-phasor dq-frame components and ρ is the reference angle of the dq-frame (Mohiuddin et al., 2016; Yazdani and Iravani, 2010); the following equations can be obtained from equation (12):

$$\dot{\imath}_{\text{d}} = -\frac{R}{L}\imath_{\text{d}} + \omega\imath_{\text{q}} - \frac{E_{\text{d}}}{L} + \frac{V_{\text{dc}}}{2L}u_{\text{d}} \quad (14a)$$

$$\dot{\imath}_{\text{q}} = -\omega\imath_{\text{d}} - \frac{R}{L}\imath_{\text{q}} - \frac{E_{\text{q}}}{L} + \frac{V_{\text{dc}}}{2L}u_{\text{q}} \quad (14b)$$

$$\dot{V}_{\text{c}} = -\frac{V_{\text{c}}}{\tau_1} - \frac{3}{4C}u_{\text{d}}\imath_{\text{d}} - \frac{3}{4C}u_{\text{q}}\imath_{\text{q}} \quad (14c)$$

If the synchronously rotating reference frame is chosen such that $E_{\text{q}} = 0$, the active and reactive power supplied to the grid can be written as:

$$P = \frac{3}{2}E_{\text{d}}\imath_{\text{d}}; \qquad Q = -\frac{3}{2}E_{\text{d}}\imath_{\text{q}} \quad (15)$$

The complete dynamical model of UCESS is represented by equation (14). The objective of the partial feedback linearizing controller is to inject active and reactive power effectively into the grid from the UCESS which can be accomplished by regulating the $\imath_{\text{d}}$ and $\imath_{\text{q}}$ components of the grid current as the grid voltage component E_{d} and E_{q} are fixed (Mohiuddin et al., 2016; Mahmud et al., 2014a). Therefore, $\imath_{\text{d}}$ and $\imath_{\text{q}}$ are selected as the control objectives for the proposed nonlinear control technique.

3. PARTIAL FEEDBACK LINEARIZABILITY OF THE UCESS

A nonlinear multi-input multi-output (MIMO) system based on the mathematical model developed in equation (14) can be written as follows:

$$\dot{x} = f(x) + g_1(x)\alpha_1 + g_2(x)\alpha_2$$
$$y_1 = h_1(x) \quad \text{and} \quad y_2 = h_2(x)$$

where $x \in \mathbb{R}^n$; $f(x)$ and $g_i(x)$ with $i = 1, 2$ are n-dimensional smooth vector fields; α_i is the i^{th} control variable, $y_i(t)$ the i^{th} output, $h_i(x)$ a scalar function of x (Lu et al., 2013). In terms of this nonlinear system, the grid-connected UCESSs can be represented as follows:

$$x = [\imath_{\text{d}}\ \imath_{\text{q}}\ V_{\text{c}}]^T \quad \text{and} \quad f(x) = \begin{bmatrix} -\frac{R}{L}\imath_{\text{d}} + \omega\imath_{\text{q}} - \frac{E_{\text{d}}}{L} \\ -\omega\imath_{\text{d}} - \frac{R}{L}\imath_{\text{q}} - \frac{E_{\text{q}}}{L} \\ -\frac{V_{\text{c}}}{\tau_1} \end{bmatrix}$$

$$g(x) = [g_1(x)\ g_2(x)] = \begin{bmatrix} \frac{V_{\text{dc}}}{2L} & 0 \\ 0 & \frac{V_{\text{dc}}}{2L} \\ -\frac{3}{4C}\imath_{\text{d}} & -\frac{3}{4C}\imath_{\text{q}} \end{bmatrix}$$

$$\alpha = \begin{bmatrix}\alpha_1 \\ \alpha_2\end{bmatrix} = \begin{bmatrix}u_{\text{d}} \\ u_{\text{q}}\end{bmatrix}; \qquad y = \begin{bmatrix}y_1 \\ y_2\end{bmatrix} = \begin{bmatrix}\imath_{\text{d}} \\ \imath_{\text{q}}\end{bmatrix}$$

Depending on the number of inputs and outputs, partial feedback linearization technique transforms a nonlinear system into a reduced order linear system or several subsystems along with an autonomous system. The dynamics of the autonomous system are also known as internal dynamics. This linearization approach can only be implemented if the total relative degree (r) of the system is less than the order (n) of the system. An overview of partial feedback linearization technique and the associated definitions can be seen in (Lu et al., 2013; Mahmud et al., 2014a).

The relative degree of the system depends on the selected output functions or control objectives. The relative degree for the output function $y_1 = h_1(x) = \imath_{\text{d}}$ and $y_2 = h_2(x) = \imath_{\text{q}}$ can be determined as follows:

$$L_g L_f^{1-1} h_1(x) = L_g h_1(x) = \frac{V_{\text{dc}}}{2L} \neq 0$$

$$L_g L_f^{1-1} h_2(x) = L_g h_2(x) = \frac{V_{\text{dc}}}{2L} \neq 0$$

which indicates that the relative degree for the output functions $h_1(x) = \imath_{\text{d}}$ is $r_1 = 1$ and also $h_2(x) = \imath_{\text{q}}$ is

$r_2 = 1$. Therefore total relative degree of the system is $r = r_1 + r_2 = 2$ and this means that $(r_1 + r_2) < n$ as $n = 3$. From the above illustration, it can be concluded that the UCESS model is partially linearized as the total relative degree of the system is less than the order. The design of a partial feedback linearizing controller for grid-connected UCESS is provided in the following section.

4. PARTIAL FEEDBACK LINEARIZING CONTROLLER DESIGN FOR UCESS SYSTEM

The necessary steps required to design the partial feedback linearizing controller are discussed in this section and the steps are as follows:

Step 1: Nonlinear coordinate transformation and partial feedback linearization of UCESS

Nonlinear coordinate transformation for the grid-connected UCESS can be defined as follows:

$$\tilde{z_1} = \tilde{\varphi}_1(x) = h_1(x) = \imath_{\mathrm{d}} \quad \text{and} \quad \tilde{z_2} = \tilde{\varphi}_2(x) = h_2(x) = \imath_{\mathrm{q}}$$

where z and x are vectors with equal dimensions and $\tilde{\varphi}$ is a nonlinear vector function of x (Lu et al., 2013). Using nonlinear coordinate transformation the partially linearized system for the UCESS can be written as follows:

$$\dot{\tilde{z_1}} = -\frac{R}{L}\imath_{\mathrm{d}} + \omega\imath_{\mathrm{q}} - \frac{E_{\mathrm{d}}}{L} + \frac{V_{\mathrm{dc}}}{2L}u_{\mathrm{d}} \tag{16a}$$

$$\dot{\tilde{z_2}} = -\omega\imath_{\mathrm{d}} - \frac{R}{L}\imath_{\mathrm{q}} - \frac{E_{\mathrm{q}}}{L} + \frac{V_{\mathrm{dc}}}{2L}u_{\mathrm{q}} \tag{16b}$$

Equation (16) can be written in the following form of a linear system:

$$\dot{\tilde{z_1}} = \tilde{v_1} \qquad \text{and} \qquad \dot{\tilde{z_2}} = \tilde{v_2}$$

where $\tilde{v_1}$ and $\tilde{v_2}$ are the linear control inputs. At this stage, any linear control approach can be employed to determine these control inputs. The linear control inputs $\tilde{v_1}$ and $\tilde{v_2}$ can be written as

$$\tilde{v_1} = -\frac{R}{L}\imath_{\mathrm{d}} + \omega\imath_{\mathrm{q}} - \frac{E_{\mathrm{d}}}{L} + \frac{V_{\mathrm{dc}}}{2L}u_{\mathrm{d}} \tag{17a}$$

$$\tilde{v_2} = -\omega\imath_{\mathrm{d}} - \frac{R}{L}\imath_{\mathrm{q}} - \frac{E_{\mathrm{q}}}{L} + \frac{V_{\mathrm{dc}}}{2L}u_{\mathrm{q}} \tag{17b}$$

Before applying control laws obtained from the partial feedback linearization, the stability of internal dynamics of the UCESS is required to check.

Step 2: Stability analysis of internal dynamics of UCESS

In Step 1, a third-order nonlinear system is transformed into two first-order decoupled subsystems representing the linear dynamics. For a stable internal dynamics, the control laws required to be chosen in such a way that the following condition is satisfied:

$$\lim_{t\to\infty} h_\imath(x) \to 0$$

which means that as the time approaches to infinity the states of the linear system decay to zero, i.e., $[\tilde{z_1}\ \tilde{z_2}\ \cdots\ \tilde{z_r}]^T \to 0$; as $t \to \infty$. For the UCESS as considered in this paper, this indicates the steady-state at which

$$\tilde{z_1} = 0 \qquad \text{and} \qquad \tilde{z_2} = 0 \tag{18}$$

The remaining nonlinear state can be represented by the nonlinear function $\hat{z} = \hat{\varphi}(x)$. To secure the stability, this needs to be selected in such a way that following constraints are satisfied:

$$L_{g1}\hat{\varphi}(x) = 0 \qquad \text{and} \qquad L_{g2}\hat{\varphi}(x) = 0 \tag{19}$$

For the UCESS, equation (19) will be satisfied if

$$\hat{\varphi}(x) = \hat{z} = -\tau_1 V_{\mathrm{c}} + \frac{1}{2}\frac{L}{V_{\mathrm{dc}}}\imath_{\mathrm{d}}^2 + \frac{1}{2}\frac{L}{V_{\mathrm{dc}}}\imath_{\mathrm{q}}^2 \tag{20}$$

Thus the remaining dynamics of the UCESS can be expressed as:

$$\dot{\hat{z}} = L_f\hat{\varphi}(x) = \frac{L}{V_{\mathrm{dc}}}\imath_{\mathrm{d}}f_1 + \frac{L}{V_{\mathrm{dc}}}\imath_{\mathrm{q}}f_2 - \tau_1 f_3 \tag{21}$$

Since $\imath_{\mathrm{d}} = h_1 = \tilde{z_1}$ and $\imath_{\mathrm{q}} = h_2 = \tilde{z_2}$ using equation (18), equation (21) can be written as:

$$\dot{\hat{z}} = V_{\mathrm{c}} \tag{22}$$

From equation (20) V_{c} can be calculated as

$$V_{\mathrm{c}} = \frac{1}{\tau_1}\left[\frac{1}{2}\frac{L}{V_{\mathrm{dc}}}\imath_{\mathrm{d}}^2 + \frac{1}{2}\frac{L}{V_{\mathrm{dc}}}\imath_{\mathrm{q}}^2 - \hat{z}\right] \tag{23}$$

Substituting $\imath_{\mathrm{d}}$ and $\imath_{\mathrm{q}}$ with $\tilde{z_1}$ and $\tilde{z_2}$ respectively and using their values from equation (18), equation (23) can be rewritten as

$$V_{\mathrm{c}} = -\frac{1}{\tau_1}\hat{z} \tag{24}$$

Finally, replacing the value of V_{c} from equation (24) into equation (22) one can derive

$$\dot{\hat{z}} = -\frac{1}{\tau_1}\hat{z} \tag{25}$$

From equation (25), it is clear that the UCESS has stable internal dynamics and hence the partial feedback linearizing controller can be implemented on such systems. From the above mentioned partial feedback linearizing scheme, it is clear that the dynamics of UCESS are divided into two parts: the external dynamics as described in the preceding step and the internal dynamics which is required to be stable for implementing the controller (Mahmud et al., 2014a).

The derivation of the proposed control law is discussed in the following step.

Step 3: Derivation of control law

For the UCESS, the original control inputs in $dq-$frame are u_{d} and u_{q} while $\tilde{v_1}$ and $\tilde{v_2}$ are linear control inputs. Using equation (17), the original control laws can be computed as:

$$u_{\mathrm{d}} = \frac{2}{V_{\mathrm{dc}}}[L\tilde{v_1} + R\imath_{\mathrm{d}} - \omega L\imath_{\mathrm{q}} + E_{\mathrm{d}}] \tag{26a}$$

$$u_{\mathrm{q}} = \frac{2}{V_{\mathrm{dc}}}[L\tilde{v_2} + \omega L\imath_{\mathrm{d}} + R\imath_{\mathrm{q}} + E_{\mathrm{q}}] \tag{26b}$$

Equation (26) is the final control law of UCESS, which controls the amount of current injected into the grid. Subsequently, the linear control inputs $\tilde{v_1}$ and $\tilde{v_2}$ are required for completing the controller design process. In this study, PI controllers are used and the structure of the two PI controllers are provided in the following:

$$\tilde{v_1} = k_{1p}(\imath_{dref} - \imath_d) + k_{1i}\int_0^t (\imath_{dref} - \imath_{\mathrm{d}})dt \tag{27a}$$

$$\tilde{v_2} = k_{2p}(\imath_{qref} - \imath_q) + k_{2i}\int_0^t (\imath_{\mathrm{qref}} - \imath_{\mathrm{q}})dt \tag{27b}$$

The gains of these PI controllers are selected in such a way that they track the reference current with a minimum amount of errors. In this study, the gains are adjusted to:

$$k_{1p} = 2\imath_{dref}, \quad k_{1i} = \imath_{dref}^2, \quad k_{2p} = 2\imath_{qref}, \quad k_{2i} = \imath_{\mathrm{qref}}^2$$

The reference values $\imath_{\mathrm{dref}}$ and $\imath_{\mathrm{qref}}$ can be determined from equation (15) (Mohiuddin et al., 2016). For a VSC, the amplitudes of modulating signals are confined to $\hat{u} \leq 1$ which need to be maintained under both steady-state and transient conditions to prevent over modulation within the system. In order to satisfy these conditions, i.e., to limit the amplitude of $\hat{u}$ under transient conditions a rate limiter is considered in this paper. The criteria for the selection of DC-bus voltage of a VSC is similar to that as presented in (Mohiuddin et al., 2016). Using the third harmonic injected PWM scheme, the amplitudes

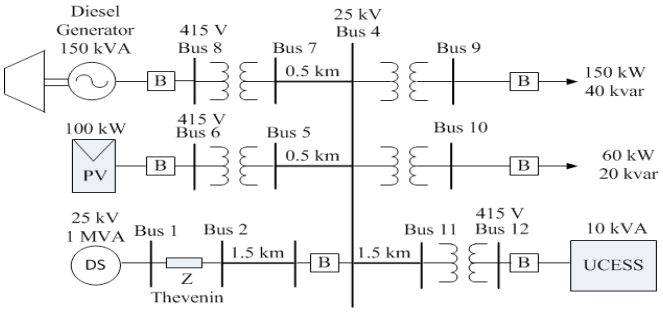

Fig. 2. Single line diagram of the 12-bus test distribution system.

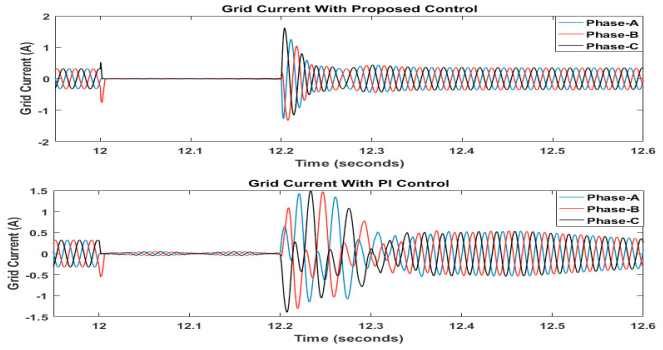

Fig. 3. Performance assessment under three-phase short circuit fault

of modulating signals can be increased by around 15 %. Therefore, a third harmonic injected PWM must satisfy the conditions $\hat{u} \leq 1.15$ under both steady-state and transient conditions which are achieved using the analysis given in (Mohiuddin et al., 2016).

5. THIRD-HARMONIC INJECTED PWM IMPLEMENTATION

From equation (5), it is clear that the values of $\hat{u}$ and $\epsilon(t)$ are required to obtain the third harmonic injected PWM modulating signals $u_{\text{aug-abc}}$. However, the partial feedback linearizing controller is designed on the dq-axes and the modulating signals u_{abc} are obtained from the control inputs u_{d} and u_{q} using dq-axes to space-phasor transformation and then space-phasor to abc-transformation. Thus, it is essential to formulate $u_{\text{aug-abc}}$ in terms of u_{abc}, u_{d}, and u_{q} (Yazdani and Iravani, 2010).

Using the trigonometric identity $\cos 3\epsilon = 4\cos^3\epsilon - 3\cos\epsilon$ in equation (5a), and then multiplying the second term in right-hand side by $\hat{u}^2/\hat{u}^2$, one can obtain:

$$u_{\text{aug-a}}(t) = \frac{3}{2}\hat{u}\cos\epsilon - \frac{2}{3}\frac{[\hat{u}\cos\epsilon]^3}{\hat{u}^2} \tag{28}$$

Substituting $\hat{u}\cos\epsilon$ with $u_{\text{a}}(t)$ from equation (4) and using $\hat{u}^2 = u_{\text{d}}^2 + u_{\text{q}}^2$ into equation (28), it can be obtained that

$$u_{\text{aug-a}}(t) = \frac{3}{2}u_{\text{a}}(t) - \frac{2}{3}\frac{u_a^3}{u_{\text{d}}^2 + u_{\text{q}}^2} \tag{29a}$$

Similarly from equations (5b) and (5c) one can write

$$u_{\text{aug-b}}(t) = \frac{3}{2}u_{\text{b}}(t) - \frac{2}{3}\frac{u_b^3(t)}{u_{\text{d}}^2 + u_{\text{q}}^2} \tag{29b}$$

$$u_{\text{aug-c}}(t) = \frac{3}{2}u_{\text{c}}(t) - \frac{2}{3}\frac{u_c^3(t)}{u_{\text{d}}^2 + u_{\text{q}}^2} \tag{29c}$$

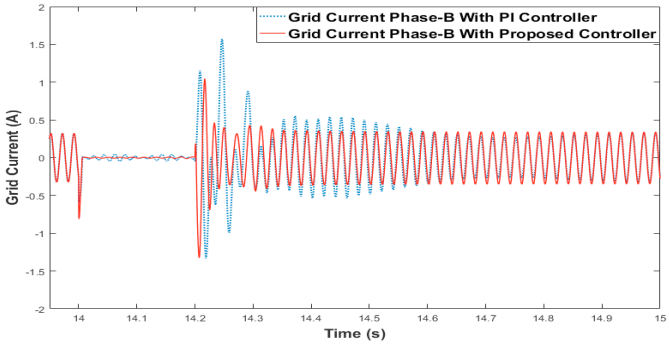

Fig. 4. Performance assessment under a single-phase short-circuit fault (red line grid current of phase B with proposed controller and blue line grid current with PI controller).

Therefore using equation (29), the third harmonic injected modulating signal can be generated through the VSC.

6. CONTROLLER PERFORMANCE ASSESSMENT

In order to assess the performance of the designed controller, the UCESS is connected to a 12-bus test distribution system as shown in Fig. 2. In this paper, a 12-bus balanced test distribution system as presented in (Mahmud et al., 2013) is considered with some modifications in the active and reactive power levels, replacement of CHP with a 150 kVA a diesel generator, and the DSTATCOM with a UCESS. In order to maintian the modulation index amplitude within unity the constraint $E_t \leq \frac{V_{\text{dc}}}{2}$ must be satisfied. Therefore, the minimum required voltage at the input of the inverter is 480 V in order to generate a phase voltage of 240 V at the output of the inverter. However, the desired 240 V phase voltage at the AC-side is obtained using only 420 V DC-bus voltage. Two different cases: faults within the system and changing load conditions are considered to demonstrate the behaviors of the system with the designed controller.

6.1 Controller performance assessment during faults within the system

In power system applications, the most severe disturbances are three-phase short-circuit faults (Mahmud et al., 2014b). In this simulation study, a symmetrical three-phase short-circuit fault with the fault sequence (fault occurs at 12 s and clears at 12.2 s) is considered at bus-11 of the test system. With this fault sequence, the post-fault currents injected into the grid with the partial feedback linearizing and the PI controller are shown in Fig. 3. A single-phase short circuit fault with the similar fault duration (fault occurs at 14 s and cleared at 14.2 s) is also considered at phase-B of the bus-11 as these forms of grid events frequently occur in the distribution system. The pre and post-fault current of phase-B under this fault sequence is depicted in Fig. 4. From Fig. 3 and Fig. 4, it is revealed that the proposed controller preserves the post-fault steady-state in a better way as compared to the PI controller.

6.2 Controller performance assessment under changing load conditions

The loads on the power system vary continuously and the controller has to track these varying loads to preserve a balance of active and reactive power demand into the

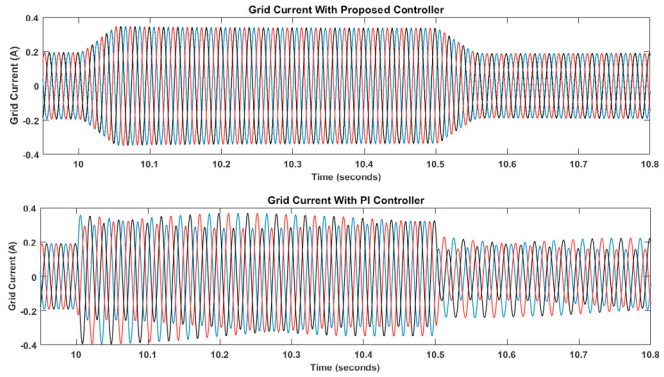

Fig. 5. Performance assessment under changing load conditions

system. In this simulation, initially it is assumed that the UCESS is tracking a 5 kVA unity power factor load. At 10 s the load changes to a 10 kVA unity power factor load for a very short duration of time (0.5 s). The controller should have the capability to regulate the switching signal of the VSC to meet the additional load demand. At 10.5 s the system again returns to its previous operating condition. For this sudden change in load the grid current injected from the UCESS is observed and provided in Fig. 5. From Fig. 5, it is clear that the designed controller has better performance in comparison to the PI-based controller.

7. CONCLUSION

A third-order harmonic injected PWM scheme is designed and implemented for a grid-connected UCESS system. Nonlinear partial feedback linearization technique is applied to control the active and reactive power injection from the UCESS where the controller is implemented after ensuring all the requirements for the design and application of the proposed approach. The objectives of eliminating nonlinearities in the system and reduction of the DC-bus voltage level is achieved which is justified through the simulation results. The proposed scheme will reduce the cost and voltage requirements of the switching devices for integrating UCESS into the microgrid as a back-up storage device. In future work, the system response will be analyzed on a practical distribution system.

REFERENCES

Abdullah, M.A., Tan, C.W., and Yatim, A.H.M. (2014). A simulation study of hybrid wind-ultracapacitor energy conversion system. In *Energy Conversion (CENCON), 2014 IEEE Conference on*, 265–270. doi: 10.1109/CENCON.2014.6967513.

Bambang, R.T., Rohman, A.S., Dronkers, C.J., Ortega, R., Sasongko, A., et al. (2014). Energy management of fuel cell/battery/supercapacitor hybrid power sources using model predictive control. *Industrial Informatics, IEEE Transactions on*, 10(4), 1992–2002.

Jang, M., Ciobotaru, M., and Agelidis, V.G. (2013). A single-phase grid-connected fuel cell system based on a boost-inverter. *Power Electronics, IEEE Transactions on*, 28(1), 279–288.

Khosravi, K., Vamegh, E., Dhaouadi, R., et al. (2015). Energy management and control of a standalone pv system using ultracapacitors. In *Electric Power and Energy Conversion Systems (EPECS), 2015 4th International Conference on*, 1–6. IEEE.

Lu, Q., Sun, Y., and Mei, S. (2013). *Nonlinear control systems and power system dynamics*, volume 10. Springer Science & Business Media.

Mahmud, M.A., Hossain, M.J., Pota, H.R., and Oo, A.M.T. (2014a). Robust nonlinear distributed controller design for active and reactive power sharing in islanded microgrids. *IEEE Transactions on Energy Conversion*, 29(4), 893–903. doi:10.1109/TEC.2014.2362763.

Mahmud, M.A., Pota, H.R., Hossain, M.J., and Roy, N.K. (2014b). Robust partial feedback linearizing stabilization scheme for three-phase grid-connected photovoltaic systems. *IEEE Journal of Photovoltaics*, 4(1), 423–431. doi:10.1109/JPHOTOV.2013.2281721.

Mahmud, M., Pota, H.R., and Hossain, M.J. (2014c). Nonlinear current control scheme for a single-phase grid-connected photovoltaic system. *Sustainable Energy, IEEE Transactions on*, 5(1), 218–227.

Mahmud, M., Pota, H., and Hossain, M. (2013). Nonlinear dstatcom controller design for distribution network with distributed generation to enhance voltage stability. *International Journal of Electrical Power & Energy Systems*, 53, 974–979.

Mohiuddin, S.M., Mahmud, M., A.M.O.Haruni, and Pota, H.R. (2016). Partial feedback linearizing control of ultracapacitor-based energy storage systems for grid-connected power system applications. In *Power System Technology (POWERCON), 2016 IEEE International Conference on*.

Molina, M.G. and Mercado, P.E. (2008). Dynamic modeling and control design of dstatcom with ultra-capacitor energy storage for power quality improvements. In *Transmission and Distribution Conference and Exposition: Latin America, 2008 IEEE/PES*, 1–8. doi: 10.1109/TDC-LA.2008.4641872.

Mor, J.J., Puleston, P.F., Kunusch, C., and Fantova, M.A. (2015). Development and implementation of a supervisor strategy and sliding mode control setup for fuel-cell-based hybrid generation systems. *IEEE Transactions on Energy Conversion*, 30(1), 218–225. doi:10.1109/TEC.2014.2354553.

Sahay, K. and Dwivedi, B. (2009). Supercapacitors energy storage system for power quality improvement: An overview. *J. Energy Sources*, 10(10), 1–8.

Sami, B.S., Abderrahmen, B.C., and Adnane, C. (2013). Design and dynamic modeling of a fuel cell/ultra capacitor hybrid power system. In *Electrical Engineering and Software Applications (ICEESA), 2013 International Conference on*, 1–7. doi:10.1109/ICEESA.2013.6578382.

Schneuwly, A. (2006). Designing auto power systems with ultracapacitors. In *Embedded Systems Conference Silicon Valley*.

Singo, T.A., Martinez, A., and Saadate, S. (2008). Using ultracapacitors to optimize energy storage in a photovoltaic system. In *Power Electronics, Electrical Drives, Automation and Motion, 2008. SPEEDAM 2008. International Symposium on*, 229–234. doi: 10.1109/SPEEDHAM.2008.4581306.

Somayajula, D. and Crow, M. (2015). An integrated active power filter-ultracapacitor design to provide intermittency smoothing and reactive power support to the distribution grid. In *2015 IEEE Power Energy Society General Meeting*, 1–1. doi: 10.1109/PESGM.2015.7286067.

Uzunoglu, M. and Alam, M.S. (2006). Dynamic modeling, design, and simulation of a combined pem fuel cell and ultracapacitor system for stand-alone residential applications. *IEEE Transactions on Energy Conversion*, 21(3), 767–775. doi:10.1109/TEC.2006.875468.

Yazdani, A. and Iravani, R. (2010). *Voltage-sourced converters in power systems: modeling, control, and applications*. John Wiley & Sons.